

NASA TECHNICAL NOTE



NASA TN D-4866

NASA TN D-4866

LOAN COPY: RE
AFWL (WLII 2091E1D
KIRTLAND AFB,

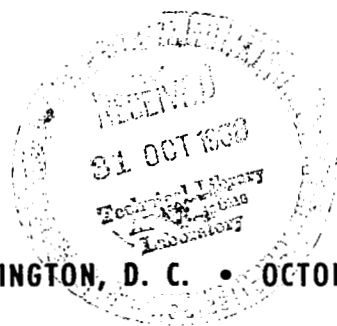


**ANALYSIS OF ELECTROMAGNETIC WAVES
ON A DIELECTRIC ROD IMMERSED IN
A PLASMA INCLUDING A DISCUSSION
OF DIAGNOSTIC APPLICATIONS**

by David L. Wright and Norman C. Wenger

*Lewis Research Center
Cleveland, Ohio*

NATIONAL AERONAUTICS AND SPACE ADMINISTRATION • WASHINGTON, D. C. • OCTOBER 1968



ANALYSIS OF ELECTROMAGNETIC WAVES ON A DIELECTRIC ROD IMMERSED IN A PLASMA INCLUDING A DISCUSSION OF DIAGNOSTIC APPLICATIONS

by David L. Wright and Norman C. Wenger

Lewis Research Center

SUMMARY

The guided electromagnetic waves that propagate along a lossless dielectric rod immersed in isotropic and uniaxial plasmas are determined. For the uniaxial plasma, only the case where the optic axis is aligned parallel to the dielectric rod is considered. Both plasmas are described by the linearized momentum transport equation for a cold, collisionless, electron fluid of uniform density. Numerical results for the propagation constants of the waves are presented as a function of the rod and plasma parameters for both the circularly symmetric and dipole modes. Important aspects of the results are discussed with particular emphasis on plasma diagnostic applications.

INTRODUCTION

During the past several years, interest in the measurement of plasma properties has been increasing. Specifically, investigations in energy conversion, electromagnetic propulsion, the reentry problem, and microwave amplifiers have created the need for accurately determining the parameters of a plasma.

Several new methods for measuring electron density are currently being investigated. One promising new method consists of relating the plasma parameters to the measurable properties of electromagnetic waves guided by a dielectric rod in the plasma. Recently, Robson and Stewart (ref. 1) presented a theoretical expression for the electron density as a function of the phase shift of the dominant HE_{11} mode along a dielectric rod in a cold, collisionless, isotropic plasma. Their experimental measurements of the electron density with this technique were approximately 30 percent higher than those obtained with a double Langmuir probe.

A more extensive investigation of wave propagation on a dielectric rod in a plasma was made by Medecki, et al. (refs. 2 and 3) for electron density measurements on the Apollo reentry flights. Their theoretical investigation considered a cold, isotropic plasma with collisions; however, numerical results were only presented for the TE_{01} mode in the collisionless case. Experimental values were obtained by placing conducting end plates on a dielectric rod to make a cylindrical probe resonator from which the electron density was obtained by observing the resonant frequency shift. Good agreement was reported between theoretical and experimental values.

Kreuzer and Müller (ref. 4) also considered electromagnetic wave propagation on a dielectric rod in a plasma. Their theoretical and experimental investigation emphasized the HE_{11} mode. They found that the phase shift of the electromagnetic waves can be made a weak function of the electron density if the rod radius is large and a strong function if it is small. A probe was constructed from a rod of large radius by narrowing a short section to a small radius. The electromagnetic waves were guided into and out of the plasma with virtually no phase shift due to the plasma on the large portion of the probe, while in the narrowed region, a measurable phase shift due to the plasma occurred from which the localized electron density was determined. Their experimental values were in good agreement with Langmuir probe data.

The previous investigators (refs. 1 to 4) have been concerned primarily with the TE_{01} or the HE_{11} mode. In this report, a formal analysis is presented for the complete set of modes that propagate along a dielectric rod in a plasma. Several of the lowest order circularly symmetric and dipole modes are investigated in detail to determine the modes and the ranges of the rod and plasma parameters that are most suitable for diagnostic applications.

Since a static magnetic field is present in many plasmas, the analysis is conducted for both isotropic and uniaxial plasmas to assess the effect of a magnetic field. In practice, a uniaxial plasma occurs whenever the electron cyclotron frequency due to the static magnetic field is much greater than the source and plasma frequencies. Only the case where the static magnetic field is aligned parallel to the dielectric rod is considered.

MODEL

The model (fig. 1) consists of an infinitely long, circular, cylindrical rod (of radius a and relative dielectric constant k) which is immersed in a cold, collisionless, homogeneous plasma. In practice, the plasma will be somewhat inhomogeneous since the electron density will be depleted near the surface of the rod because of the formation of a plasma sheath. The sheath region, which can be approximated by a thin layer of free space, can easily be taken into account when $k = 1$. The net effect in this case is

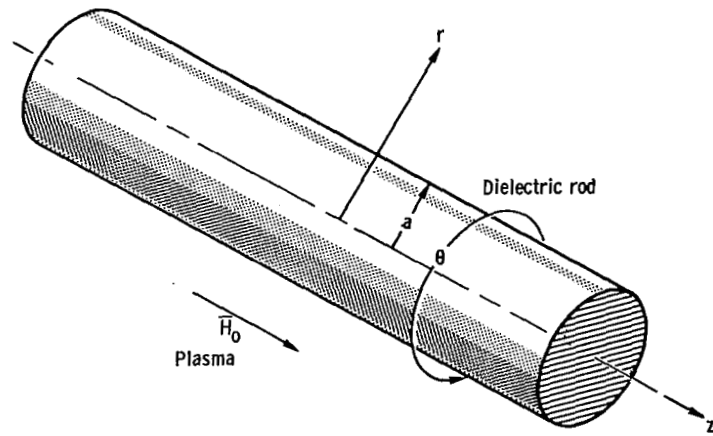


Figure 1. - Dielectric rod in plasma.

simply to increase the rod radius by the sheath thickness since the rod and sheath have the same value of dielectric constant. However, the effect of the sheath when k is other than 1 cannot be taken into account as readily. Thus, to simplify the analysis, the effect of the sheath will be omitted.

GENERAL SOLUTION FOR FIELD

Basic Equations

The basic equations to be used are Maxwell's equations and the linearized momentum transport equation for a cold, collisionless, electron fluid with an applied static magnetic field. These equations are

$$\nabla \times \bar{e} = -j\omega\mu_0 \bar{h} \quad (1)$$

$$\nabla \times \bar{h} = qN_0 \bar{v} + j\omega\epsilon_0 \bar{e} \quad (2)$$

$$j\omega m_e \bar{v} = q(\bar{e} + \bar{v} \times \mu_0 \bar{H}_0) \quad (3)$$

where

\bar{e} time-varying electric field

\bar{H}_0 static magnetic field

\bar{h} time-varying magnetic field

m_e	mass of electron
N_o	equilibrium electron density
q	charge of electron
\bar{v}	electron fluid velocity vector
ϵ_0	permittivity of free space
μ_0	permeability of free space
ω	angular source frequency

It has been assumed that the time variation of all nonstationary quantities is $e^{j\omega t}$, where ω is sufficiently large that the ion motion can be neglected. Equations (1) to (3) can be combined to yield

$$\nabla \times \bar{e} = -j\omega \mu_0 \bar{h} \quad (4)$$

$$\nabla \times \bar{h} = j\omega \epsilon_0 \bar{\bar{K}} \cdot \bar{e} \quad (5)$$

If the static magnetic field is either weak so that $\omega_c \ll \omega_p$ and $\omega_c \ll \omega$ (isotropic plasma) or strong so that $\omega_c \gg \omega_p$ and $\omega_c \gg \omega$ (uniaxial plasma), the relative permittivity tensor or dyad $\bar{\bar{K}}$ for the static magnetic field in the z-direction is given by

$$\bar{\bar{K}} = \epsilon_1 (\hat{a}_r \hat{a}_r + \hat{a}_\theta \hat{a}_\theta) + \epsilon_p \hat{a}_z \hat{a}_z \quad (6)$$

ϵ_1	ϵ_p for an isotropic plasma and $\epsilon_1 = 1$ for a uniaxial plasma and
ϵ_p	relative dielectric constant of isotropic plasma, $1 - (\omega_p^2/\omega^2)$
ω_c	angular electron cyclotron frequency, $ q\mu_0 H_0/m_e $
ω_p^2	square of angular plasma frequency, $q^2 N_o / \epsilon_0 m_e$
\hat{a}_i	unit vector in i^{th} direction

Note that equations (4) and (5) also apply in an ordinary dielectric medium with a relative dielectric constant k if $\bar{\bar{K}}$ is replaced by $k\bar{I}$, where \bar{I} is the unit dyad.

General Solution of Basic Equations in Plasma

The solutions sought in this problem are electromagnetic waves guided by the rod which vary as $e^{-j\beta z}$ along the z-axis, where β is the propagation constant. These so-

solutions for the electric and magnetic fields are derived by first finding the solutions for the z-component of the fields from which the transverse components are then obtained.

The electric and magnetic fields can be expressed in component form as

$$\bar{e} = (\bar{e}_t + e_z \hat{a}_z) e^{-j\beta z} \quad (7)$$

$$\bar{h} = (\bar{h}_t + h_z \hat{a}_z) e^{-j\beta z} \quad (8)$$

where

e_z time-varying axial electric field

\bar{e}_t time-varying transverse electric field

h_z time-varying axial magnetic field

\bar{h}_t time-varying transverse magnetic field

Likewise, the operator ∇ can be expressed as

$$\nabla = \nabla_t + \frac{\partial}{\partial z} \hat{a}_z$$

where ∇_t is the transverse operator (in cylindrical coordinates $\nabla_t = \hat{a}_r(\partial/\partial_r)$ $+ (\hat{a}_\theta/r)(\partial/\partial_\theta)$).

Substituting equations (7) and (8) into equations (4) and (5) and equating like components yield

$$\nabla_t \times \bar{h}_t = j\omega\epsilon_0 \epsilon_p e_z \hat{a}_z \quad (9)$$

$$\nabla_t \times h_z \hat{a}_z - j\beta \hat{a}_z \times \bar{h}_t = j\omega\epsilon_0 \epsilon_1 \bar{e}_t \quad (10)$$

$$\nabla_t \times \bar{e}_t = -j\omega\mu_0 h_z \hat{a}_z \quad (11)$$

$$\nabla_t \times e_z \hat{a}_z - j\beta \hat{a}_z \times \bar{e}_t = -j\omega\mu_0 \bar{h}_t \quad (12)$$

Now, solving equation (12) for \bar{h}_t and substituting this result into equation (10) yield

$$\bar{e}_t = \frac{j}{\alpha^2} (\omega\mu_0 \nabla_t \times h_z \hat{a}_z + \beta \hat{a}_z \times \nabla_t \times e_z \hat{a}_z) \quad (13)$$

where

$$\alpha = \left(\beta^2 - \epsilon_1 k_o^2 \right)^{1/2} \quad (14)$$

$$k_o = \frac{\omega}{c}$$

$$c = \frac{1}{(\epsilon_0 \mu_0)^{1/2}} \quad (\text{speed of light in a vacuum})$$

The transverse electric field \bar{e}_t can be expressed in radial and azimuthal component form as

$$e_r = \frac{j}{\alpha^2} \left(\frac{\omega \mu_0}{r} \frac{\partial h_z}{\partial \theta} + \beta \frac{\partial e_z}{\partial r} \right) \quad (15)$$

and

$$e_\theta = \frac{j}{\alpha^2} \left(-\omega \mu_0 \frac{\partial h_z}{\partial r} + \frac{\beta}{r} \frac{\partial e_z}{\partial \theta} \right) \quad (16)$$

Next, substituting equation (13) into (12) to eliminate \bar{e}_t yields

$$\bar{h}_t = \frac{j}{\omega \mu_0 \alpha^2} \left[\alpha^2 \nabla_t \times e_z \hat{a}_z + \beta \hat{a}_z \times \left(\omega \mu_0 \nabla_t \times h_z \hat{a}_z + \beta \hat{a}_z \times \nabla_t \times e_z \hat{a}_z \right) \right] \quad (17)$$

The transverse magnetic field \bar{h}_t can be written in radial and azimuthal component form as

$$h_r = \frac{j}{\alpha^2} \left(-\omega \epsilon_0 \epsilon_1 \frac{\partial e_z}{\partial \theta} + \beta \frac{\partial h_z}{\partial r} \right) \quad (18)$$

and

$$h_\theta = \frac{j}{\alpha^2} \left(\omega \epsilon_0 \epsilon_1 \frac{\partial e_z}{\partial r} + \frac{\beta}{r} \frac{\partial h_z}{\partial \theta} \right) \quad (19)$$

The differential equation for h_z is obtained by substituting equation (13) into (11) to eliminate \bar{e}_t ; this yields

$$\left(\nabla_t^2 - \alpha^2 \right) h_z = 0 \quad (20)$$

where ∇_t^2 is the transverse Laplacian (in cylindrical geometry $\nabla_t^2 = (\partial^2/\partial r^2) + (1/r)(\partial/\partial r) + (1/r^2)(\partial^2/\partial \theta^2)$). Likewise, the differential equation for e_z is obtained by substituting equation (17) into (9) which yields

$$\left(\nabla_t^2 - \delta^2 \right) e_z = 0 \quad (21)$$

where

$$\delta = \left[\left(\frac{\epsilon_p}{\epsilon_1} \right) \left(\beta^2 - \epsilon_1 k_o^2 \right) \right]^{1/2} \quad (22)$$

The general solutions for equations (20) and (21) are readily found to be

$$h_z = \sum_{n=-\infty}^{\infty} A_n K_n(\alpha r) e^{jn\theta} e^{j\omega t} \quad (23)$$

$$e_z = \sum_{n=-\infty}^{\infty} B_n K_n(\delta r) e^{jn\theta} e^{j\omega t} \quad (24)$$

where

n azimuthal wave number

$K_n(x)$ modified Bessel function of n^{th} order

A_n constant to be determined

B_n constant to be determined

Since the fields must vanish as $r \rightarrow \infty$, the branch of the square root in equations (14)

and (22) that has a positive real part must be chosen for the radial wave numbers α and δ . Substituting equations (23) and (24) into (15), (16), (18), and (19) yields the general solutions for the transverse components of \bar{e} and \bar{h} .

General Solution of Basic Equations in Dielectric

As previously indicated in the section Basic Equations, the fields in a dielectric can be expressed by the plasma equations if the relative dielectric tensor $\bar{\bar{K}}$ is replaced by $k\bar{I}$. Thus, equations (20) and (21) yield

$$\left(\nabla_t^2 + \alpha_0^2\right)h_z = 0 \quad (25)$$

and

$$\left(\nabla_t^2 + \alpha_0^2\right)e_z = 0 \quad (26)$$

respectively, where the z-dependence of the fields is assumed to be of the form $e^{-j\beta z}$ and

$$\alpha_0 = \left(kk_0^2 - \beta^2\right)^{1/2} \quad (27)$$

The general solutions to equations (25) and (26) are

$$h_z = \sum_{n=-\infty}^{\infty} C_n J_n(\alpha_0 r) e^{jn\theta} e^{j\omega t} \quad (28)$$

$$e_z = \sum_{n=-\infty}^{\infty} D_n J_n(\alpha_0 r) e^{jn\theta} e^{j\omega t} \quad (29)$$

where

$J_n(x)$ Bessel function of n^{th} order

C_n constant to be determined

D_n constant to be determined

Either sign of the square root in equation (27) may be chosen.

The transverse components for the fields in the dielectric can be obtained by substituting equations (28) and (29) into equations (15), (16), (18), and (19) with α^2 replaced by $-\alpha_0^2$, and ϵ_1 replaced by k .

Dispersion Equation

The boundary conditions require e_z , h_z , e_θ , and h_θ to be continuous at the surface of the rod. These conditions lead to the following dispersion equation

$$\left(\frac{n\beta}{k_0 a}\right)^2 \left(\frac{1}{\alpha_0^2} + \frac{1}{\alpha^2}\right)^2 = \left[\frac{J'_n(\alpha_0 a)}{J_n(\alpha_0 a)} + \frac{K'_n(\alpha a)}{K_n(\alpha a)} \right] \left\{ k \left[\frac{J'_n(\alpha_0 a)}{J_n(\alpha_0 a)} \right] + \epsilon_1 \left[\delta \frac{K'_n(\delta a)}{K_n(\delta a)} \right] \right\} \quad (30)$$

where the prime refers to differentiation with respect to the total argument.

The solutions for β are, in general, both real and complex; however, only the real values of β which satisfy the dispersion equation will be presented since this analysis is only concerned with unattenuated propagating waves. It should also be noted that equation (30) is an even function of both β and n . Thus, the spectrum of waves that propagates along the positive z -axis is identical to that which propagates along the negative z -axis; likewise, the spectrum of left circularly polarized waves is identical to that of the right circularly polarized waves. Hence, it is not necessary to investigate explicitly the dispersion equation for negative values of β and n .

NUMERICAL RESULTS AND DISCUSSION

The results are presented starting with the simplest limiting case of a dielectric rod in free space. Next, the results for a dielectric rod in an isotropic plasma are presented, and finally the results for a dielectric rod in a uniaxial plasma are considered.

These results are presented in the form of curves for the dimensionless propagation constant βa as a function of the dimensionless source frequency $k_0 a$ for various dimensionless plasma frequencies $\omega_p a/c$. The values of the dielectric constant used are 1, 2, and 10.

Except in the circularly symmetric case ($n = 0$), the waves that correspond to the various solutions for βa are hybrids; that is, all three components of the electric and magnetic field are present. These hybrid waves are denoted as either electric hybrid (EH) or magnetic hybrid (EH). Each hybrid wave can be considered to be the sum of a transverse electric (TE) and transverse magnetic (TM) wave, with the TE component being dominant in the EH wave and the TM component being dominant in the HE wave.

In order to determine whether a particular solution for βa corresponds to an EH or HE wave, the limiting case where $\omega_p a/c$ is infinite is considered. This limit reduces the model to an ordinary, dielectric filled, circular, waveguide where all the waves are TE and TM. If a particular hybrid wave reduces to a TE in this limit, the hybrid wave is denoted by EH; if it reduces to a TM, it is denoted by HE. As previously mentioned, the circularly symmetric waves are not hybrids; all these solutions correspond to TE and TM waves.

In addition, each wave is further denoted by the subscripts n and m which signify the azimuthal and radial orders of the wave, respectively. Values for these subscripts are selected so that in the limiting case where $\omega_p a/c$ is infinite they coincide with the subscripts of the corresponding circular waveguide modes.

Dielectric Rod in Free Space

The dispersion equation for a dielectric rod in free space can be obtained from equation (30) with $\epsilon_1 = \epsilon_p = 1$. For the circularly symmetric case ($n = 0$), the dispersion equation reduces to

$$\frac{k\alpha_1 a K_0(\alpha_1 a)}{K_1(\alpha_1 a)} + \frac{\alpha_0 a J_0(\alpha_0 a)}{J_1(\alpha_0 a)} = 0 \quad (31)$$

and

$$\frac{\alpha_1 a K_0(\alpha_1 a)}{K_1(\alpha_1 a)} + \frac{\alpha_0 a J_0(\alpha_0 a)}{J_1(\alpha_0 a)} = 0 \quad (32)$$

where

$$\alpha_1 a = \left[(\beta a)^2 - (k_0 a)^2 \right]^{1/2} \quad (33)$$

It can be shown that solutions of equations (31) and (32) correspond to TM_{om} and TE_{om} modes, respectively. For the dipole case ($n = 1$), equation (30) reduces to

$$\left\{ \frac{-1}{(\alpha_1 a)^2} \left[\frac{\alpha_1 a K_0(\alpha_1 a)}{K_1(\alpha_1 a)} + 1 \right] + \frac{1}{(\alpha_0 a)^2} \left[\frac{\alpha_0 a J_0(\alpha_0 a)}{J_1(\alpha_0 a)} - 1 \right] \right\} \left\{ \frac{-1}{(\alpha_1 a)^2} \left[\frac{\alpha_1 a K_0(\alpha_1 a)}{K_1(\alpha_1 a)} + 1 \right] \right. \\ \left. + \frac{k}{(\alpha_0 a)^2} \left[\frac{\alpha_0 a J_0(\alpha_0 a)}{J_1(\alpha_0 a)} - 1 \right] \right\} = \left(\frac{\beta a}{k_0 a} \right)^2 \left[\frac{1}{(\alpha_0 a)^2} + \frac{1}{(\alpha_1 a)^2} \right]^2 \quad (34)$$

The solutions of equation (34) correspond to both EH_{1m} and HE_{1m} modes.

Before the numerical results for the dispersion equations are presented, it is worthwhile to consider the region in the $(\beta a - k_0 a)$ plane where solutions can exist. For a dielectric rod in free space, solutions to the dispersion equations are possible only if the $K_n(\alpha_1 a)$ function is real. This only occurs if the argument $\alpha_1 a$ is real; consequently, βa is bounded from below by the line $\beta a = k_0 a$. Moreover, it can be shown by considering the sign of each term in the dispersion equations that βa is bounded from above by the line $\beta a = k^{1/2} k_0 a$. These bounds are shown in figure 2 and are valid for all values of n .

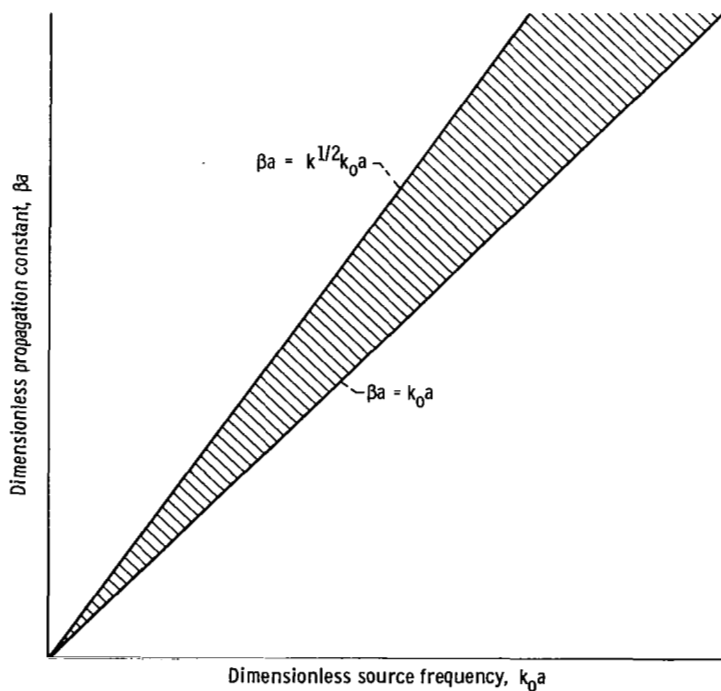
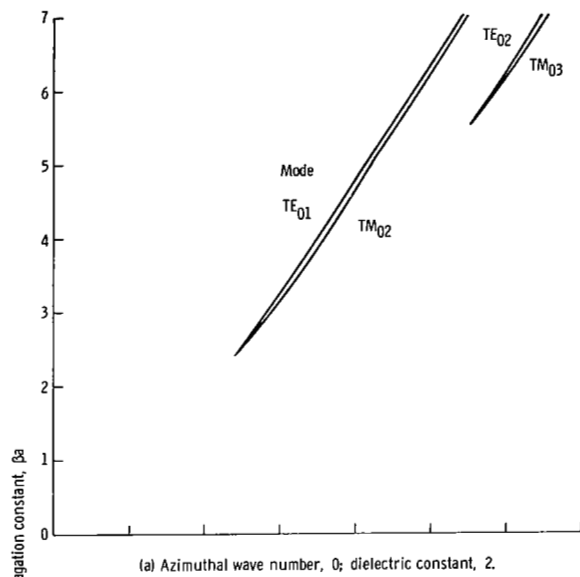
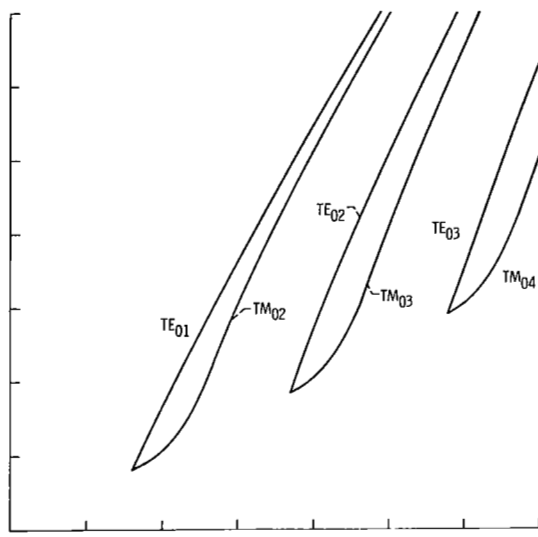


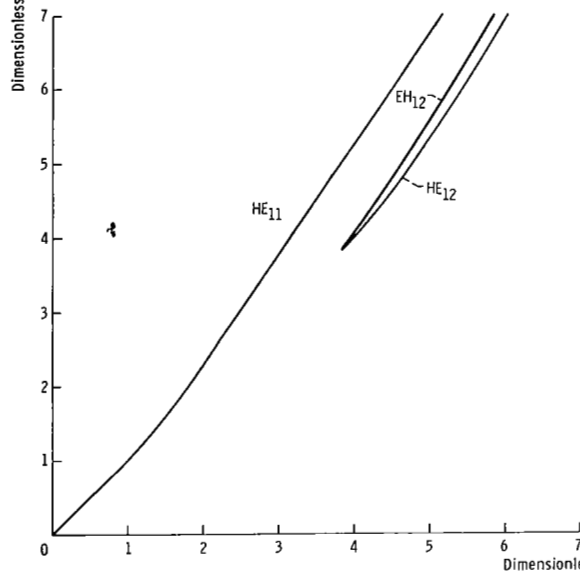
Figure 2. - Region of solutions for dielectric rod in free space.



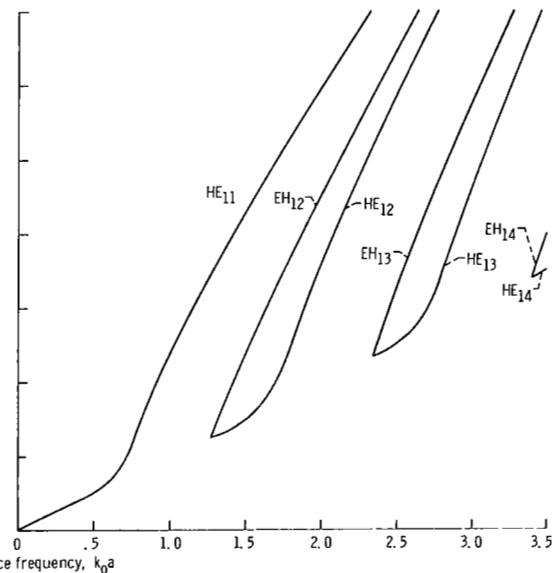
(a) Azimuthal wave number, 0; dielectric constant, 2.



(b) Azimuthal wave number, 0; dielectric constant, 10.



(c) Azimuthal wave number, 1; dielectric constant, 2.



(d) Azimuthal wave number, 1; dielectric constant, 10.

Figure 3. - Dielectric rod in free space.

There are, of course, no solutions to the dispersion equations for a dielectric rod in free space if $k = 1$. Numerical results for $k = 2$ and $k = 10$ are presented in figure 3. Note that the TM_{01} and the EH_{11} modes (as defined on p. 10) do not exist for the dielectric rod in free space.¹

¹In the literature on surface waveguides (see, e. g., ref. 5) the TM_{02} mode as defined in this report is often called the TM_{01} mode, the TM_{03} mode is often called the TM_{02} mode, etc.

The results show that all modes except the HE_{11} have a low frequency cutoff which occurs on the line $\beta a = k_o a$. For the case $n = 0$, it can be shown that the only values for βa and $k_o a$ on this line which satisfy equations (31) and (32) are given by $\alpha_o a = [k(k_o a)^2 - (\beta a)^2]^{1/2} = \sigma_{om}$ where σ_{om} is the m^{th} zero of $J_o(\sigma_{om})$ ($\sigma_{01} = 2.405$, $\sigma_{02} = 5.520 \dots$). Thus, the lower cutoff frequency for the TE_{om} and $TM_{o(m+1)}$ modes is

$$k_o a = \frac{\sigma_{om}}{(k - 1)^{1/2}} \quad (35)$$

For the case $n = 1$, the lower cutoff frequency obtained from equation (34) for the $EH_{1(m+1)}$ and $HE_{1(m+1)}$ modes is

$$k_o a = \frac{\sigma_{1m}}{(k - 1)^{1/2}} \quad (36)$$

where σ_{1m} is the m^{th} zero of $J_1(\sigma_{1m})$ ($\sigma_{10} = 0.0$, $\sigma_{11} = 3.832 \dots$). There are no upper cutoff frequencies for modes on a dielectric rod in free space; as $k_o a$ increases, the value of βa for each mode asymptotically approaches $k^{1/2} k_o a$.

Dielectric Rod in Isotropic Plasma

The dispersion equation for a dielectric rod in an isotropic plasma is given by equation (30) with $\epsilon_1 = \epsilon_p$. For $n = 0$ it yields

$$\frac{k \alpha_2 a K_o(\alpha_2 a)}{K_1(\alpha_2 a)} + \frac{\epsilon_p \alpha_o a J_o(\alpha_o a)}{J_1(\alpha_o a)} = 0 \quad (37)$$

for TM_{om} modes and

$$\frac{\alpha_2 a K_o(\alpha_2 a)}{K_1(\alpha_2 a)} + \frac{\alpha_o a J_o(\alpha_o a)}{J_1(\alpha_o a)} = 0 \quad (38)$$

for TE_{om} modes where

$$\alpha_2 a = \left[(\beta a)^2 - \epsilon_p (k_o a)^2 \right]^{1/2} \quad (39)$$

For $n = 1$ it yields

$$\left\{ \frac{-1}{(\alpha_2 a)^2} \left[\frac{\alpha_2 a K_0(\alpha_2 a)}{K_1(\alpha_2 a)} + 1 \right] + \frac{1}{(\alpha_0 a)^2} \left[\frac{\alpha_0 a J_0(\alpha_0 a)}{J_1(\alpha_0 a)} - 1 \right] \right\} \left\{ \frac{-\epsilon_p}{(\alpha_2 a)^2} \left[\frac{\alpha_2 a K_0(\alpha_2 a)}{K_1(\alpha_2 a)} + 1 \right] \right. \\ \left. + \frac{k}{(\alpha_0 a)^2} \left[\frac{\alpha_0 a J_0(\alpha_0 a)}{J_1(\alpha_0 a)} - 1 \right] \right\} = \left(\frac{\beta a}{k_o a} \right)^2 \left[\frac{1}{(\alpha_0 a)^2} + \frac{1}{(\alpha_2 a)^2} \right]^2 \quad (40)$$

for EH_{1m} and HE_{1m} modes. The region in the $(\beta a - k_o a)$ plane where solutions to the dispersion equations exist for an isotropic plasma is shown in figure 4. It can be shown that if $k_o a < \omega_p a/c$, all values of βa are allowed. If $k_o a > \omega_p a/c$, βa is bounded from above by the line $\beta a = k^{1/2} k_o a$ and from below by the curve $\beta a = [(\kappa_o a)^2 - (\omega_p a/c)^2]^{1/2}$. These bounds are valid for all values of n .

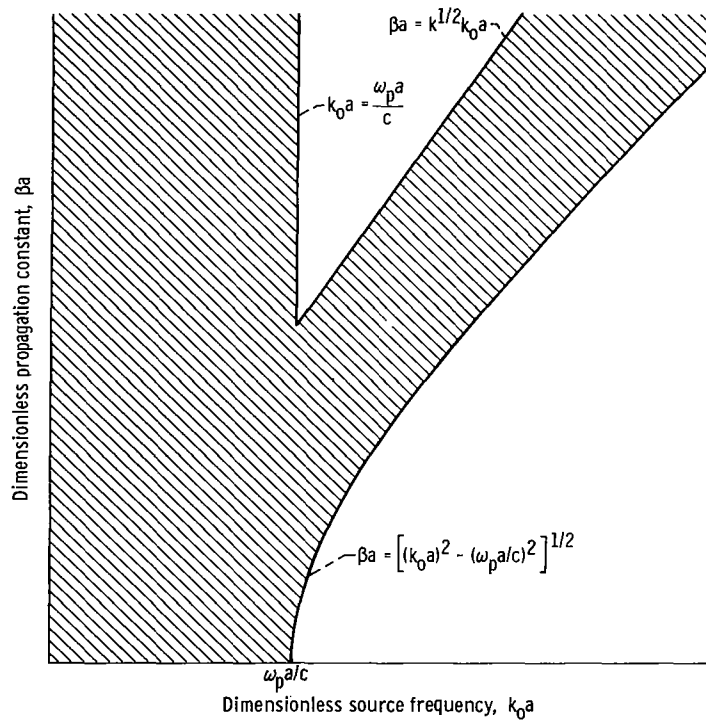


Figure 4. - Region of solutions for dielectric rod in plasma.

Numerical results for a dielectric rod in an isotropic plasma are presented in figure 5. It should be noted from figures 5(d) to (i) that the presence of the plasma allows the TM_{01} and EH_{11} modes to propagate in contrast to the free-space case where they are cut off. The dispersion curves for these modes approach the line $k_o a = 0$ as $\omega_p a/c$ becomes small.

For low plasma frequencies, both the TM_{01} and EH_{11} modes are backward waves. This is particularly well illustrated in figures 5(d) to (f) for the TM_{01} mode with $\omega_p a/c = 1$. As the plasma frequency increases, these modes change from backward to forward waves. However, this transition does not occur at a discrete plasma frequency, but rather over a narrow range. If the dispersion curves for these modes are examined on a greatly magnified scale in this range, it is found that they are double valued with one value corresponding to a forward wave and the other to a backward wave. For the TM_{01} mode, this narrow range can be approximated by a discrete plasma frequency which is given by

$$\frac{\omega_p a}{c} \approx 2.4 \left(\frac{k+1}{2k} \right)^{1/2} \quad (41)$$

This equation was obtained from equation (37) by equating the value of $k_o a$ for infinite βa to the value of $k_o a$ for $\beta a = k^{1/2} k_o a$. For the case shown in figures 5(d) to (f) where $k = 1, 2$, and 10 , these plasma frequencies are $\omega_p a/c = 2.4, 2.1$, and 1.8 , respectively. No suitable criterion exists which yields a simple expression for approximating this narrow range of plasma frequencies for the EH_{11} mode.

As $k_o a$ approaches the value

$$k_o a = \frac{\frac{\omega_p a}{c}}{(k+1)^{1/2}} \quad (42)$$

the value of βa for the TM_{01} and EH_{11} modes approaches infinity. This value of $k_o a$ corresponds to a low-frequency cutoff for backward waves and a high-frequency cutoff for forward waves. Conversely, the high-frequency cutoff for backward waves and the low-frequency cutoff for forward waves cannot be expressed as simply since they involve the solutions of the transcendental dispersion equations (37) and (40).

The dispersion curves for the remaining modes shown in figure 5 always correspond to forward waves. Except in the special case where $k = 1$, which is treated separately, these curves are similar for low values of plasma frequency such as $\omega_p a/c = 1.0$ since they are merely perturbations of the free-space case. For higher plasma frequencies

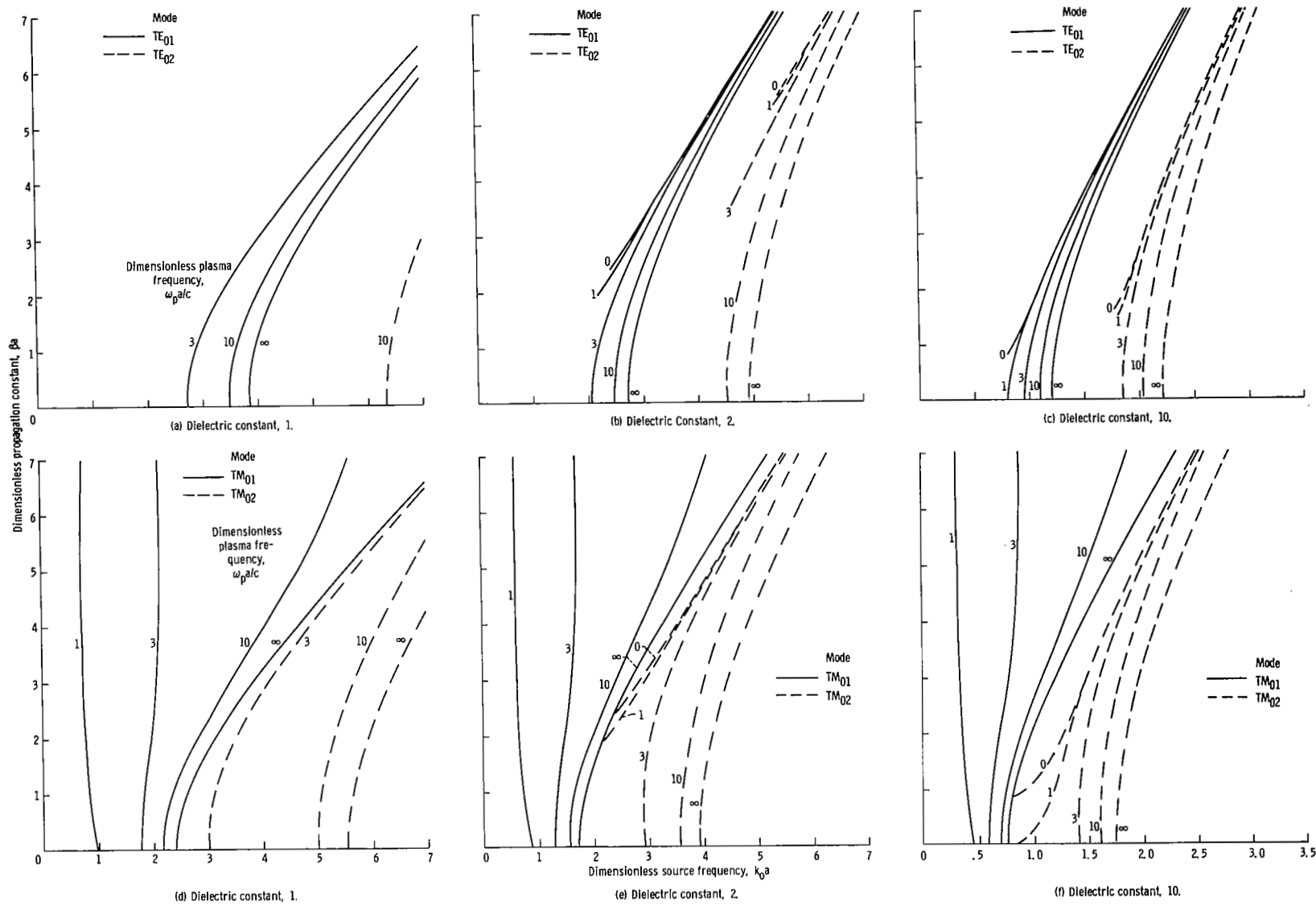


Figure 5. - Dielectric rod in isotropic plasma.

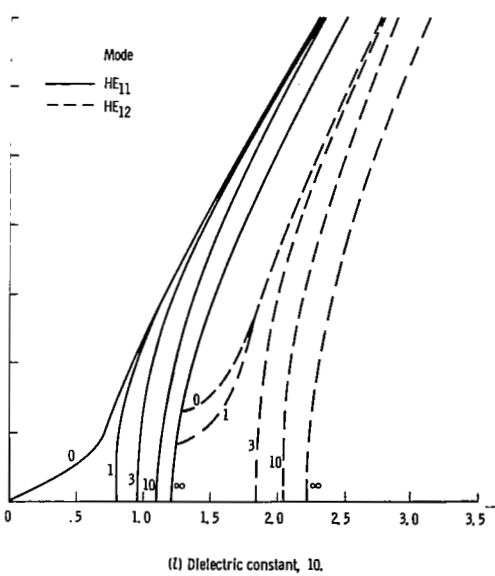
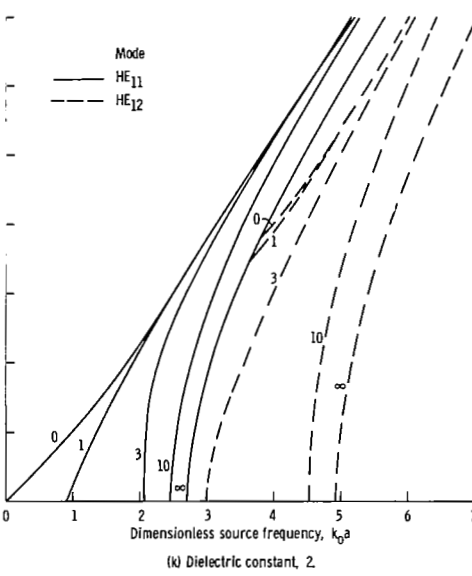
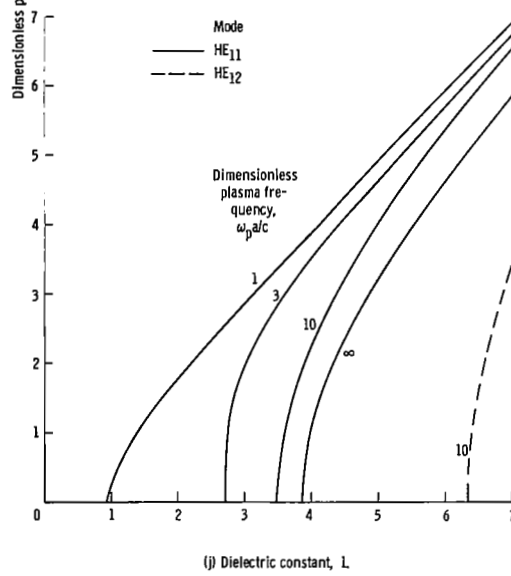
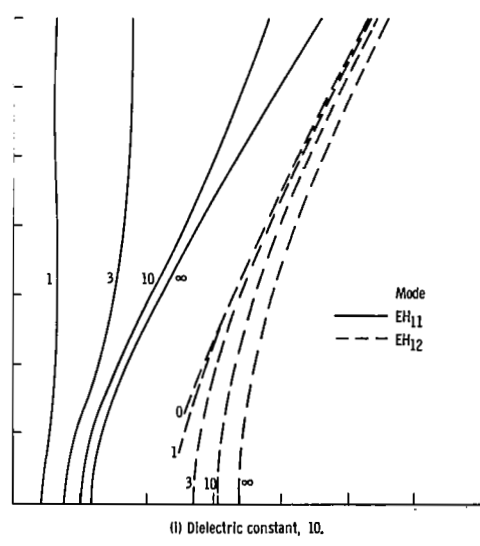
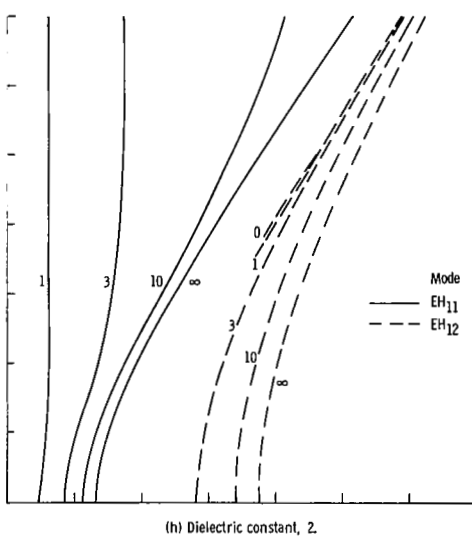
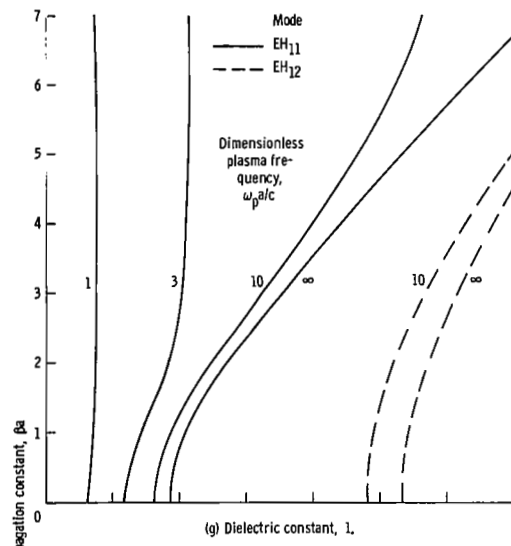


Figure 5. - Concluded.

such as $\omega_p a/c = 10.0$, the curves approach those for a dielectric filled circular waveguide; for $\omega_p a/c = \infty$ the curves are, of course, identical to those for a dielectric filled circular waveguide.

Each of these modes has a lower cutoff frequency but no upper cutoff frequency. As $k_o a$ becomes large, the value of β_a for each mode asymptotically approaches $k^{1/2} k_o a$ as in the free-space case. This is physically understandable since the effect of the plasma is negligible if $k_o a \gg \omega_p a/c$. For all these modes except the HE_{11} , the low-frequency cutoff first decreases with increasing $\omega_p a/c$ until a critical value for $\omega_p a/c$ is reached and then continuously increases with increasing $\omega_p a/c$. For values of $\omega_p a/c$ below the critical plasma frequency, the low-frequency cutoff is given by

$$k_o a = \left[\frac{\left(\sigma_{om}\right)^2 - \left(\frac{\omega_p a}{c}\right)^2}{k - 1} \right]^{1/2} \quad (43)$$

for the TE_{om} and $TM_{o(m+1)}$ modes and

$$k_o a = \left[\frac{\left(\sigma_{1m}\right)^2 - \left(\frac{\omega_p a}{c}\right)^2}{k - 1} \right]^{1/2} \quad (44)$$

for the $EH_{1(m+1)}$ and $HE_{1(m+1)}$ modes. At the critical plasma frequency, cutoff occurs at $k_o a = \omega_p a/c$, where $\omega_p a/c$ is given by

$$\frac{\omega_p a}{c} = \frac{\sigma_{om}}{k^{1/2}} \quad (45)$$

for the TE_{om} and $TM_{o(m+1)}$ modes and

$$\frac{\omega_p a}{c} = \frac{\sigma_{1m}}{k^{1/2}} \quad (46)$$

for the $HE_{1(m+1)}$ and $EH_{1(m+1)}$ modes. For values of $\omega_p a/c$ above the critical plasma frequency, the low-frequency cutoff for each mode is obtained by solving the appropriate transcendental dispersion equation with $\beta a = 0$. For the HE_{11} mode, the low-frequency cutoff is zero for $\omega_p a/c = 0$ and continuously increases with increasing plasma frequency.

For the special case where $k = 1$, there are no solutions to the dispersion equation other than the TM_{01} and EH_{n1} modes unless the plasma frequency exceeds a critical value. It can be shown that this value is given by equations (45) and (46) for $n = 0$ and 1, respectively. For $k = 1$, all modes other than the TM_{01} and EH_{n1} modes have a lower but no upper cutoff frequency as in the case for general k . As $k_o a$ becomes large, the value of βa asymptotically approaches the value of $k_o a$. The lower cutoff frequency for each mode continuously increases as $\omega_p a/c$ increases, with the minimum value of the lower cutoff frequency being equal to the critical plasma frequency.

Dielectric Rod in Uniaxial Plasma

The dispersion equation for a dielectric rod in a uniaxial plasma with the optic axis (i. e., direction of strong static magnetic field) aligned parallel to the rod is given by equation (30) with $\epsilon_1 = 1$. For $n = 0$ it yields

$$\frac{k(\alpha_1 a)^2 K_0(\delta_1 a)}{(\delta_1 a) K_1(\delta_1 a)} + \frac{\alpha_0 a J_0(\alpha_0 a)}{J_1(\alpha_0 a)} = 0 \quad (47)$$

for TM_{0m} modes and

$$\frac{\alpha_1 a K_0(\alpha_1 a)}{K_1(\alpha_1 a)} + \frac{\alpha_0 a J_0(\alpha_0 a)}{J_1(\alpha_0 a)} = 0 \quad (48)$$

for TE_{0m} modes where

$$\delta_1 a = \left\{ \epsilon_p \left[(\beta a)^2 - (k_o a)^2 \right] \right\}^{1/2} \quad (49)$$

and for $n = 1$ it yields

$$\left\{ \left[\frac{\alpha_0 a J_0(\alpha_0 a)}{J_1(\alpha_0 a)} - 1 \right] - \left[\frac{\alpha_1 a K_0(\alpha_1 a)}{K_1(\alpha_1 a)} + 1 \right] \right\} \left\{ k \left[\frac{\alpha_0 a J_0(\alpha_0 a)}{J_1(\alpha_0 a)} - 1 \right] - \left[\frac{\delta_1 a K_0(\delta_1 a)}{K_1(\delta_1 a)} + 1 \right] \right\} = \left(\frac{\beta a}{k_0 a} \right)^2 \left[\frac{1}{(\alpha_0 a)^2} + \frac{1}{(\alpha_1 a)^2} \right]^2 \quad (50)$$

for EH_{1m} and HE_{1m} modes.

The regions in the $(\beta a - k_0 a)$ plane where solutions to the dispersion equations can exist for the uniaxial plasma are shown in figure 6. It can be shown that if $k_0 a > \omega_p a/c$, solutions for all modes (i. e., all values of n) exist in the region which is bounded from below by the line $\beta a = k_0 a$ and from above by $\beta a = k^{1/2} k_0 a$. These bounds are identical to those for the free-space case. When $k_0 a < \omega_p a/c$ only the circularly symmetric modes can exist. For the TE_{0m} modes, the upper and lower bounds on βa are $\beta a = k^{1/2} k_0 a$ and $\beta a = k_0 a$, respectively. For the TM_{0m} modes, the upper and lower

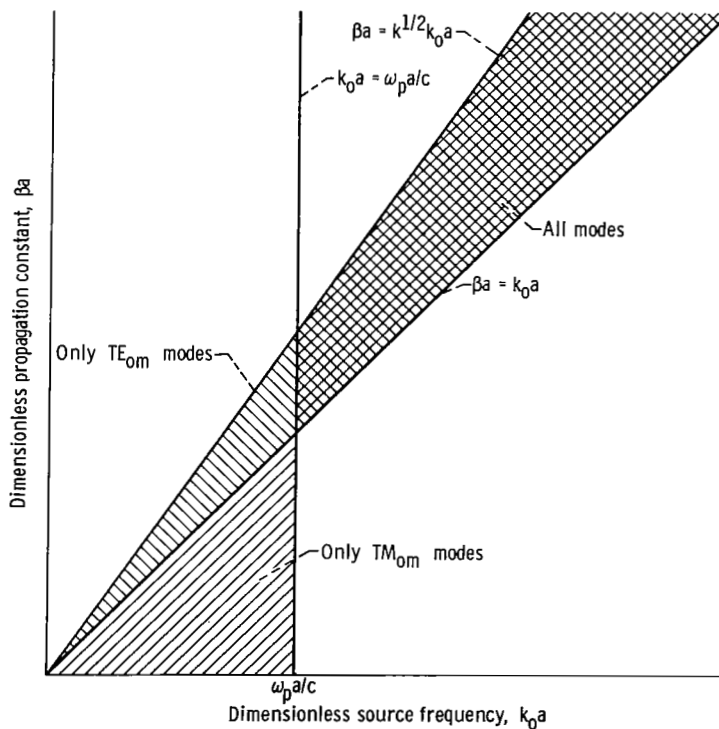


Figure 6. - Region of solutions for dielectric rod in uniaxial plasma.

bounds are $\beta a = k_o a$ and $\beta a = 0$, respectively. It should be noted that if $k = 1$, only TM_{om} modes can exist and then only for $k_o a < \omega_p a/c$.

Comparing equation (48) with (32) reveals that the dispersion equations for the TE_{om} modes are identical for the uniaxial and free-space cases. This result should be expected since the electrons in a uniaxial plasma can only move parallel to the static magnetic field which is in the z -direction, and the TE_{om} modes, by definition, have no component of electric field in this direction. Thus, there is no interaction between the plasma and the TE_{om} modes for the uniaxial case.

Numerical results for the TM_{om} modes are given in figure 7. First, consider these results for $k = 1$. The TM_{01} mode for the uniaxial case exists for all values of $\omega_p a/c$ and has both a lower and an upper cutoff frequency as in the isotropic plasma case. The lower cutoff frequency can be obtained from equation (47) with $\beta a = 0$; the upper cutoff frequency occurs along the line $\beta a = k_o a$ at $k_o a = \omega_p a/c$. The $TM_{o(m+1)}$ modes ($m \geq 1$) exist only if $\omega_p a/c \geq \sigma_{1m}$. They also have both upper and lower cutoff frequencies. The lower cutoff frequencies for the $TM_{o(m+1)}$ modes are given by equation (47) with $\beta a = 0$, where the lowest possible value for the $(m + 1)^{th}$ mode is $k_o a = \sigma_{1m}$. The upper cutoff frequency occurs at $k_o a = \omega_p a/c$, where the value of βa at the upper cutoff frequency is

$$\beta a = [(k_o a)^2 - (\sigma_{1m})^2]^{1/2}.$$

Next, consider the case where the dielectric constant k is greater than 1; for this case, the TM_{om} modes exist for all values of $\omega_p a/c$. Again, the TM_{01} mode has both an upper and lower cutoff frequency. The lower cutoff frequency is obtained as before by setting $\beta a = 0$ in equation (47). The upper cutoff frequency occurs along the line $\beta a = k_o a$ at $k_o a = \omega_p a/c$ if $\omega_p a/c < \sigma_{01}/(k - 1)^{1/2}$, and at $k_o a = \sigma_{01}/(k - 1)^{1/2}$ if $\omega_p a/c > \sigma_{01}/(k - 1)^{1/2}$. The results for the $TM_{o(m+1)}$ modes ($m \geq 1$) differ from the TM_{01} modes since they have a lower but no upper cutoff frequency. Discussion of the lower cutoff frequencies can be divided into three cases. For $\omega_p a/c < \sigma_{om}/(k - 1)^{1/2}$, the cutoff occurs on the line $\beta a = k_o a$ at $k_o a = \sigma_{om}/(k - 1)^{1/2}$. For $\sigma_{om}/(k - 1)^{1/2} < \omega_p a/c < \sigma_{1m}/k^{1/2}$, the cutoff occurs on the line $\beta a = k_o a$ at $k_o a = \omega_p a/c$. Finally, for $\omega_p a/c > \sigma_{1m}/k^{1/2}$, the cutoff can be obtained from equation (47) by setting $\beta a = 0$.

The dispersion curves for the $TM_{o(m+1)}$ modes ($m \geq 1$) are interesting since they have discontinuities or gaps in both βa and $k_o a$. For $\sigma_{1m}/k^{1/2} < \omega_p a/c < \sigma_{o(m+1)}/(k - 1)^{1/2}$, a gap in βa occurs at $k_o a = \omega_p a/c$. For a given $\omega_p a/c$ in this range, the upper and lower values of βa at the gap are the maximum and minimum values of $[k(\omega_p a/c)^2 - (\sigma_{1m})^2]^{1/2}$ and $\omega_p a/c$, respectively. Note that the gap vanishes

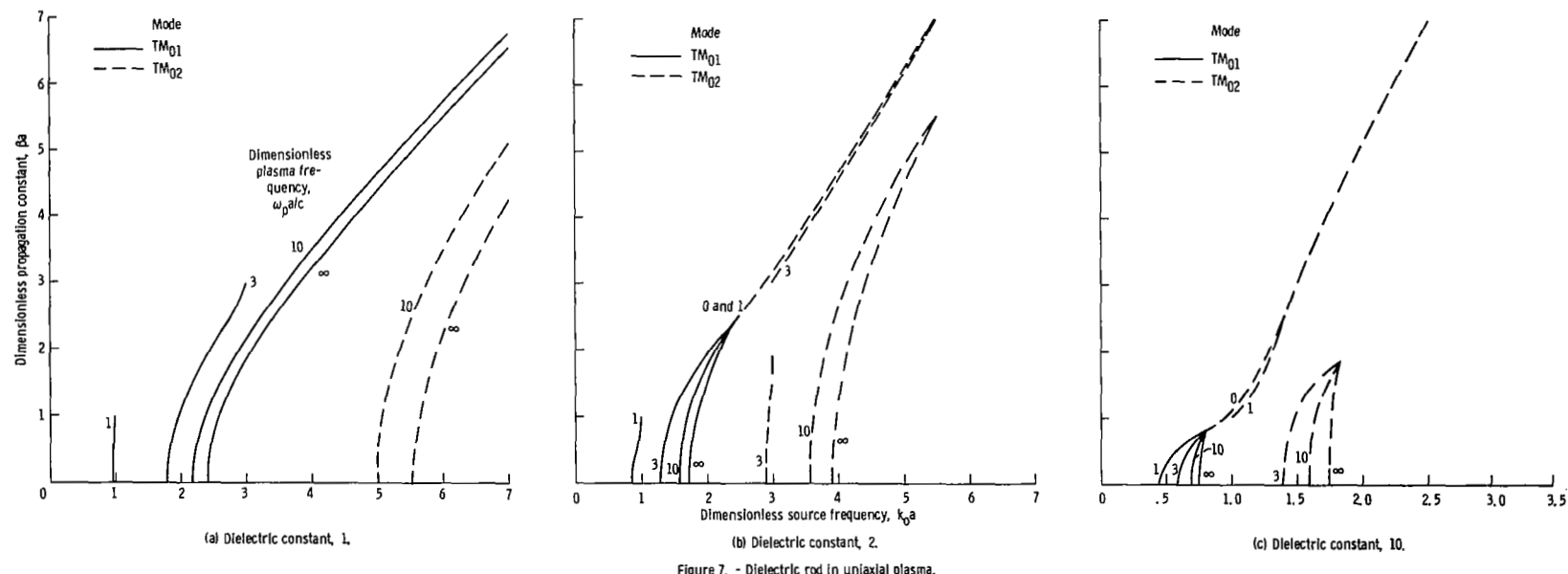


Figure 7. - Dielectric rod in uniaxial plasma.

for $\omega_p a/c = \sigma_{1m}/(k - 1)^{1/2}$. For $\omega_p a/c > \sigma_{0(m+1)}/(k - 1)^{1/2}$, the gap occurs both in βa and $k_o a$. The lower coordinates of the gap are $\beta a = \sigma_{1(m+1)}/(k - 1)^{1/2}$ and $k_o a = \sigma_{1(m+1)}/(k - 1)^{1/2}$; the upper coordinates are $\beta a = [k(\omega_p a/c)^2 - (\sigma_{1m})^2]^{1/2}$ and $k_o a = \omega_p a/c$.

Numerical results were also computed for the dipole modes in the uniaxial plasma. In the region of the $(\beta a - k_o a)$ plane where these solutions exist, the dipole solutions are practically indistinguishable from the corresponding dipole solutions for the free-space case. This is understandable since solutions for the case $n = 1$ cannot exist if $k_o a < \omega_p a/c$ (see fig. 6) where the strongest interaction between electromagnetic waves and the plasma normally occurs. If $k_o a > \omega_p a/c$, the strong static magnetic field completely eliminates the interaction of the plasma with the transverse electric field. Thus, only the axial component of the electric field can interact with the plasma. This interaction is apparently small since the solutions are almost identical to those for the free-space case.

APPLICATION OF RESULTS

Dielectric rods in plasmas have been used to determine electron density in two basic ways. The first consists of terminating a short section of rod of length L with conducting end plates to form a resonator (refs. 2 and 3). This structure will resonate when the value of $k_o a$ is such that the corresponding value of βa is an integral multiple of $\pi a/L$. These values of $k_o a$ are indicative of the electron density.

To facilitate the discussion of this method, it is useful to define a sensitivity S_r as the rate of change of the resonant frequency with respect to the plasma frequency at a fixed propagation constant or

$$S_r = \left. \frac{\partial(\omega)}{\partial(\omega_p)} \right|_{\beta=\text{constant}} = \left. \frac{\partial(k_o a)}{\partial\left(\frac{\omega_p a}{c}\right)} \right|_{\beta a=\text{constant}} \quad (51)$$

In order for the resonator method to be useful, the sensitivity must exceed a minimum value. For example, assume that a change in resonant frequency of 0.1 percent can be resolved. Then, if a change in electron density of 5 percent is to be detected, the sensitivity S_r must exceed $4 \times 10^{-2}(\omega/\omega_p)$.

The second method of determining the electron density consists of a direct measurement of the phase shift βL between points spaced a distance L along a dielectric rod in

a plasma (refs. 1 and 4). This measurement is normally conducted at a fixed source frequency $k_o a$. The sensitivity of this method S_φ is defined as the rate of change of the phase shift with respect to the plasma frequency at a fixed source frequency or

$$S_\varphi = \left. \frac{\partial(\beta L)}{\partial(\omega_p)} \right|_{\omega=\text{constant}} = \left. \frac{L}{c} \frac{\partial(\beta a)}{\partial\left(\frac{\omega_p a}{c}\right)} \right|_{k_o a=\text{constant}} \quad (52)$$

To determine an approximate lower limit on the sensitivity S_φ , consider an example where the minimum phase shift that can be resolved is 0.1 radian and where it is desirable to detect a 5 percent change in electron density. This will require S_φ to exceed $4/\omega_p$.

The dynamic range for either of these methods is the range of $\omega_p a/c$ over which the sensitivity is sufficiently high to give the desired resolution in the electron density.

The spatial resolution of the electron density measurement depends on the dimensions of the rod and the penetration of the electromagnetic field into the plasma. The spatial resolution in the axial direction is equal, of course, to the length L . The spatial resolution in the radial direction depends on the radius of the rod a and the dimensionless radial wave numbers αa and δa . It can be shown from the asymptotic forms for the modified Bessel functions in equations (29) and (30) that if $\alpha a \geq 1$ and $\delta a \geq 1$, the total radial extent of the axial electric field is of the order of $a[1 + (1/\delta a)]$ and the total radial extent of the axial magnetic field is of the order of $a[1 + (1/\alpha a)]$. If $\alpha a \ll 1$ and $\delta a \ll 1$, the radial extents of the axial electric and magnetic fields are generally quite large with respect to the radius of the rod. Thus, to obtain good spatial resolution it is necessary to select solutions where αa and δa are at least 1 and a and L are small.

The basic objective when applying the results, therefore, is to select the mode of propagation, values for the radius and dielectric constant of the rod, and values for either βa or $k_o a$, that maximize the sensitivity and yet maintain the desired spatial resolution and dynamic range.

First, consider the results for the isotropic plasma presented in figure 5. The TM_{01} and EH_{11} modes appear to be very suitable for use in the resonator technique because they yield a high sensitivity and a large dynamic range. Moreover, their sensitivities are nearly independent of the rod radius and plasma frequency if the value chosen for βa is larger than the value of the largest dimensionless plasma frequency of interest. For large values of βa , the sensitivity is the same for both the TM_{01} and EH_{11} modes and can easily be computed using equation (51) giving $S_r = 1/(k + 1)^{1/2}$. This value is 25 times greater than the minimum value required for the example on page 23.

Since βa is of the order of $\pi a/L$, both a and L can be small and still give the required value for βa . Thus, good spatial resolution can be obtained with these modes since the values of αa and δa , which are of the order of βa in this case, are large and a and L can be made small.

The HE_{11} mode also appears to be useful in the resonator technique. For this mode, small values of βa and $\omega_p a/c$ give the largest sensitivity; however, the electromagnetic field may have a large radial extent since αa and δa can be small if βa and $\omega_p a/c$ are small. For larger values of βa , the sensitivity is generally very low unless $\omega_p a/c$ is between 1 and 10. To obtain values in this range requires a prohibitively large rod radius for low plasma frequencies. For example, if the electron density N_o is 10^{15} per cubic meter, the rod radius must be of the order of 1.7×10^{-1} to 1.7 meters; however, if N_o is 10^{19} per cubic meter, the rod radius must only be of the order of 1.7×10^{-3} to 1.7×10^{-2} meters.

For the remaining modes, the value of βa in most applications must be made larger than the value of βa at the low-frequency cutoff for the free-space case to ensure that resonance will occur for all values of $\omega_p a/c$. Such a value for βa will generally yield good spatial resolution but a low sensitivity unless $\omega_p a/c$ can be made large. Again, this may result in a prohibitively large rod radius. Thus, the TM_{01} and EH_{11} modes appear to be the most suitable for use in the resonator technique - especially for the measurement of low plasma frequencies with good spacial resolution.

All modes except the TM_{01} and EH_{11} modes appear to be useful in the phase shift method. However, the source frequency for a particular mode must be selected sufficiently high so that the mode will propagate over the range of $\omega_p a/c$ of interest. Maximum sensitivity generally occurs for values of $\omega_p a/c$ in the range from 1 to 10. To achieve values in this range will require a large rod radius and hence give poor radial spatial resolution if the plasma frequency is low. If $\omega_p a/c$ is restricted to be small, the sensitivity in the phase shift method can still be made arbitrarily large by increasing the length L (see eq. (52)). This can be done, however, only at the expense of decreased axial spatial resolution. Thus, the phase shift method is generally not useful for measuring low electron densities with good spatial resolution.

For the uniaxial case, only the TM_{0m} modes are useful; these modes are shown in figure 7. The TM_{01} mode appears to be usable in the resonance technique if the value chosen for βa is less than the value of $\omega_p a/c$ for the lowest plasma frequency of interest. In this region, the sensitivity is high, particularly for low plasma frequencies. Moreover, the sensitivity is nearly independent of the rod radius as in the isotropic case.

The TM_{02} mode is usable in the resonator technique only for special cases since the dispersion curves are not a continuous function of $\omega_p a/c$. The usefulness of the TM_{02} mode is further restricted since the sensitivity is low unless the value of $\omega_p a/c$ is large which may require a large rod radius if the plasma frequency is low. Thus, the TM_{01}

mode appears to be the most suitable for use in the resonator technique for the uniaxial case.

The uniaxial TM_{01} and TM_{02} modes appear to be very restricted in their usefulness in the phase shift method. The TM_{01} mode gives a high sensitivity and generally adequate spatial resolution but only over a very small dynamic range. It may be possible to extend the dynamic range, however, by operating at several different source frequencies. The TM_{02} mode gives a large dynamic range and adequate radial spatial resolution for low values of $\omega_p a/c$; however, the sensitivity is very low unless the axial spatial resolution is sacrificed by making L large. For large values of $\omega_p a/c$, the sensitivity is generally adequate, but the dynamic range is limited and the spatial resolution may be poor especially if the plasma frequency is low. Thus, the TM_{01} also appears to be the most suitable for use in the phase shift method for the uniaxial case.

The parameter that has not yet been explicitly considered is k , the relative dielectric constant of the rod. A study of the results in figures 5 and 7 reveals that varying k produces two main effects. First, as k increases, the maximum sensitivity decreases for either technique discussed. This decrease is generally accompanied, however, by an increase in the dynamic range. Thus, the selection of the dielectric constant can be used advantageously to trade off sensitivity for dynamic range or the converse. The second main effect due to varying k is that either the source or resonant frequencies can be scaled with the scaling factor being approximately $1/k^{1/2}$. This effect can be used in some cases to bring the frequency of interest within the range of available instrumentation. Furthermore, by properly choosing k it may be possible to bring the radial extent of the field within acceptable limits.

In addition to the selection of the rod and plasma parameters, several other factors must be considered before using electromagnetic wave propagation on a dielectric rod as a plasma diagnostic tool. One of these is mode identification. A general source for electromagnetic waves will excite not only the circularly symmetric and dipole modes, but also the quadrupole ($n = 2$) and higher modes. Thus, it is necessary to select a source configuration that will preferentially excite the mode or modes of interest so that they can be easily identified. This is particularly important when either the TM_{01} or EH_{11} mode is used in an isotropic plasma since these modes along with the EH_{n1} ($n = 2, 3, \text{ etc.},$) modes have their respective dispersion curves in the same region of the $(\beta a - k_0 a)$ plane.

Another factor to be considered is the effect of the inhomogeneous region in the plasma near the surface of the rod. As noted in the section MODEL, its effect for $k = 1$ is simply to increase the effective rod radius by approximately the thickness of this sheath. Since the sheath thickness is often unknown, it may be advantageous to operate where the relation between the wave and plasma parameters is not a strong function of the

rod radius. This is best illustrated by the resonator method with either the TM_{01} or EH_{11} mode.

CONCLUDING REMARKS

The guided electromagnetic waves that propagate along a lossless dielectric rod immersed in both an isotropic and uniaxial plasma were determined. Numerical solutions were presented for the propagation constants as a function of the parameters of the model for both the circularly symmetric and dipole modes.

For the isotropic plasma, the TM_{01} and EH_{11} modes were generally the most suitable for use in the resonator method. They had good sensitivity, even for low electron densities, and a large dynamic range. For the phase shift method, all modes except the TM_{01} and EH_{11} were acceptable; however, the values for the dimensionless plasma frequencies generally had to be in the range from 1 to 10 to give maximum sensitivity, which could result in poor spatial resolution if the plasma frequency is low.

For the uniaxial case, only the TM_{0m} modes proved to be usable. The TM_{01} mode appeared to be the most suitable for use in the resonance technique if the value chosen for the propagation constant was less than the lowest value of interest for the dimensionless plasma frequency. The TM_{02} mode was only usable for special applications because of discontinuities in the dispersion curves. Both the TM_{01} and TM_{02} modes were limited in their usefulness in the phase shift method. The TM_{01} mode had a limited dynamic range which could, however, be expanded by operating at several different source frequencies. The TM_{02} mode generally had either inadequate sensitivity or poor spatial resolution unless the electron density was high.

Lewis Research Center,
National Aeronautics and Space Administration,
Cleveland, Ohio, July 16, 1968,
125-24-03-05-22.

APPENDIX - SYMBOLS

A_n, B_n	see eqs. (23) and (24)	k_o	ω/c (free-space wave number)
C_n, D_n	see eqs. (28) and (29)	L	length of dielectric rod used as probe (for resonance technique, L is distance between conducting end plates; for phase shift method, L is distance over which phase shift is measured)
a	radius of dielectric rod (see fig. 1)	m_e	mass of electron
\hat{a}_i	unit vector in i^{th} direction	N_o	equilibrium electron density
c	speed of light in vacuum	q	charge of electron
e_r	time-varying radial electric field	r	radial coordinate (see fig. 1)
e_z	time-varying axial electric field	S_r	sensitivity of resonator method (see eq. (51))
e_θ	time-varying azimuthal electric field	S_φ	sensitivity of phase shift method (see eq. (52))
\bar{e}	time-varying electric field	t	time
\bar{e}_t	time-varying transverse electric field	\bar{v}	electron fluid velocity vector in plasma
\bar{H}_o	static magnetic field	z	axial coordinate (see fig. 1)
h_r	time-varying radial magnetic field	α	$(\beta^2 - \epsilon_1 k_o^2)^{1/2}$
h_z	time-varying axial magnetic field	α_o	$(k k_o^2 - \beta^2)^{1/2}$
h_θ	time-varying azimuthal magnetic field	$\alpha_1 a$	$[(\beta a)^2 - (k_o a)^2]^{1/2}$
\bar{h}	time-varying magnetic field	$\alpha_2 a$	$[(\beta a)^2 - \epsilon_p (k_o a)^2]^{1/2}$
\bar{h}_t	time-varying transverse magnetic field	β	propagation constant in z -direction
\bar{I}	unit dyad	δ	$[(\epsilon_p / \epsilon_1)(\beta^2 - \epsilon_1 k_o^2)]^{1/2}$
$J_n(x)$	Bessel function of n^{th} order	δ_1	$\left\{ \epsilon_p [(\beta a)^2 - (k_o a)^2] \right\}^{1/2}$
$K_n(x)$	modified Bessel function of n^{th} order		
\bar{K}	relative permittivity tensor of plasma (see eq. (6))		
k	relative dielectric constant rod		

ϵ_0	permittivity of free space	σ_{1m}	m^{th} zero of $J_1(x)$
ϵ_p	relative dielectric constant of isotropic plasma	ω	angular source frequency
ϵ_1	see eq. (6)	ω_c	angular electron cyclotron frequency
μ_0	permeability of free space	ω_p	angular plasma frequency
θ	coordinate in azimuthal direction (see fig. 1)	Subscripts:	
σ_{om}	m^{th} zero of $J_0(x)$	m	order of mode in radial direction
		n	azimuthal wave number

REFERENCES

1. Robson, P. N.; and Stewart, R. D.: Surface-Wave Probe for Measuring Electron Densities in a Gaseous Plasma. *Electronics Letters*, vol. 1, no. 1, Mar. 1965, pp. 13-14.
2. Medecki, Hector; and Attwood, David: Development of an Electron Density Probe. Tech. Rep. -594, General Applied Science Labs., Inc. (NASA CR-84150), June 26, 1966.
3. Medecki, Hector; Abele, Manlio; and Attwood, David: K-Band Electron Density Probe. Tech. Rep. -662, General Applied Science Labs., Inc. (NASA CR-91382), May 25, 1967.
4. Kreuzer, H. J.; Müller, K. G.: Dielektrische Wellenleiter als Plasmasonden. *Zeit. f. Physik*, vol. 200, no. 5, 1967, pp. 541-555.
5. Barlow, H. M.; and Brown, J.: Radio Surface Waves. Clarendon Press, Oxford, 1962.